Numerical research of measurements of Shack-Hartmann wavefront sensor according to the parameters of its optical parts and the intensity of turbulent distortions

N.V. Goleneva[ab], V. Lavrinov [a], L.N. Lavrinova* [a 1]
[a] V.E. Zuev Institute of Atmospheric Optics SB RAS, 1, Academician Zuev square, Tomsk, 634021, Russia; [b]Tomsk State University, 36, Lenina Avenue, Tomsk, 634050, Russia

ABSTRACT

The wavefront sensor of Hartmann type consists of two parts: the optical and algorithmic. The parameters of the optical part of the sensor may vary. Since the time of "frozen" turbulence due to the Fried's length and to the cross wind transport turbulent distortion speed, the measurement Shack-Hartmann sensor depend on the intensity of turbulent distortions. In this paper are presented the results of the analysis of the measurements of the sensor according to the size of lens array and to the intensity of turbulent distortions. The analysis is performed on basis of a numerical model of the Shack-Hartmann wavefront sensor and on Kolmogorov's turbulence model.

Keywords: coordinates of the centroid, Shack–Hartmann wavefront sensor, turbulent atmosphere

1. INTRODUCTION

The development of adaptive optics began in 70-80th of 20th century and was stimulated primarily by such tasks for the successful solution of which is necessary to eliminate the disturbance of the wavefront [1] caused by uncontrolled random effects. One of the first measuring element adaptive optical system (AOS) was a Shack-Hartmann wavefront sensor (S-H WFS) [2], which can be divided into two parts: the algorithmic and optical. Optical part S-H WFS consists of a lens array and high-resolution video camera which is installed in the plane of the image registration.

S-H WFS is one of the main elements of the phase-conjugate AOS is not inferior to the complexity of the adaptive mirror. Initially, the sensor was designed for astronomical telescopes in which it was necessary to measure the wavefront distortions, caused by atmospheric turbulence, and eliminate jitter of star images. Development of adaptive optics was leading to changes in the sensor assembly. The main elements of the latest developments of Hartmann sensor type are microlens screen and high-resolution video camera. Replacement of the S-H WFS elementary lens pattern on the fragment of the off-axis diffractive lens with the same focal point, but substantially larger diameter [2], provided the conditions for working with beams that are able to register the accumulation of atmospheric wavefront distortions from the artificial Star created by a laser.

The optical part of the S-H WFS consists of lens array (micro-lens matrix) and high-resolution video camera that is mounted in the plane of the image registration (Fig. 1). Arriving at the entrance aperture of the sensor the wavefront is divided into a finite number of subapertures. At each subaperture the wavefront slope is estimated at measured displacements of the power centers of gravity of the focal spots (centroids), the coordinates of which are calculated, for example, by the equations [2]:

$$\xi_n = \sum_{i=1}^{n_i} iI_i \Big/ \sum_{i=1}^{n_i}\sum_{j=1}^{n_j} I_{ij}\,,\quad \eta_n = \sum_{j=1}^{n_j} jI_j \Big/ \sum_{i=1}^{n_i}\sum_{j=1}^{n_j} I_{ij}\,,\quad I_i = \sum_{j=1}^{n_j} I_{ij}\,,\quad I_j = \sum_{i=1}^{n_i} I_{ij}\,, \tag{1}$$

where I_{ij} – the measured values of the signal intensity for the element with the coordinates i, j; $i = 1,2,...n_i$;

*lnl@iao.ru; phone (3822) 491372; fax (3822) 492086

[1]This work was supported by a grant from the Russian Science Foundation №15-19-20013

21st International Symposium on Atmospheric and Ocean Optics: Atmospheric Physics,
edited by G. G. Matvienko, O. A. Romanovskii, Proc. of SPIE Vol. 9680, 96802F
© 2015 SPIE · CCC code: 0277-786X/15/$18 · doi: 10.1117/12.2205591

Downloaded From: http://proceedings.spiedigitallibrary.org/ on 11/24/2015 Terms of Use: http://spiedigitallibrary.org/ss/TermsOfUse.aspx

$j = 1,2,...n_j$; n_i, n_j – the number of pixel on subaperture corresponding to the element; $n = 1,2,..., N_{lens} \cdot N_{lens}$ – the index of subaperture; $N_{lens} \cdot N_{lens}$ – the number of subapertures. Coordinates of centroids ξ, η are expressed in radians through the picture on the video camera. Shack–Hartmann pattern consists of images of focal spots in the registration plane by video camera.

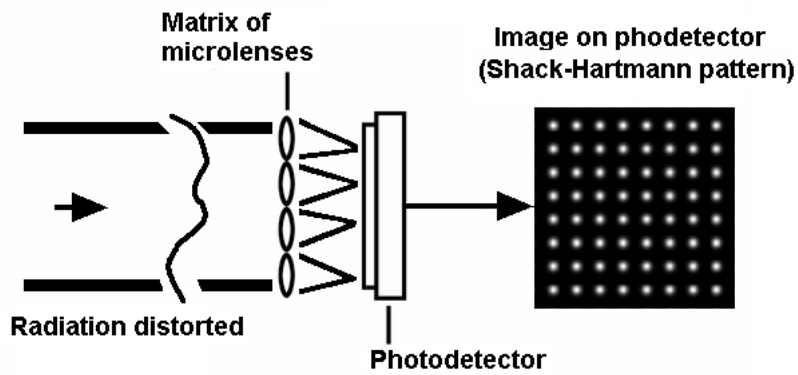

Fig.1. Opto-electronic scheme of the S-H WFS.

S-H WFS is widely used because of its compactness, resistance to vibration [3]. Based on his measurements in the AOS are being reconstructed wavefront [3, 4], the definition of the structure function of the refractive index [5], as well as the determination of the speed of the transverse component of the wind transport of atmospheric turbulence [6].

On the centroid coordinates measured by sensor is reconstructed the wavefront, which is used to control the management flexible mirror in AOS. There are many ways of wavefront reconstruction, for example, method, based on Karhunen-Loève imperfections [7, 8], method of neural networks [4].

According to the traditional approach to the reconstruction the wave function $W(x, y)$ is represented as an expansion in Zernike's polynomials [9]: $W(x, y) = \sum_{i=1}^{N} c_i Z_i(x, y)$, where c_i – the weight coefficients. Adapting local slopes this expansion to estimates derived in S-H WFS is realized by the method of least squares [10].

An important problem in the performers of AOS is the delay in the feedback loop due to a break the time of the registration by sensor of wavefront distortion and the time of correction their by flexible mirror. Reduction of influence of the time delay can be implemented by advanced adaptive correction, which are - in applying to the mirror control actions calculated relative wavefront measured at the moment that wavefront , built on a projected measurements of sensor [11, 12]. This method of reducing the impact of the delay on the accuracy of its work requires knowledge of wind speed on the input aperture of the system. The calculation of the transverse components of wind speed based on the use of the correlation properties of the data measured by the sensor, which was first demonstrated Roddier back in 1973 [13]. The authors [14, 15] also used the hypothesis of the expansion of phase change in a Taylor series to determine the speed of the cross wind transfer of turbulence.

It is known [16] that the time of "frozen" turbulence, i.e. the time during which the phase relationships change only under the influence of the wind, associated with a the Fried's length r_0 and of the transverse component of wind speed v_x by the expression: $\tau_0 = 0{,}31 r_0 / v_x$.

During τ_0 the turbulent inhomogeneities move a distance $0{,}31 r_0$. The parameter r_0 characterizes the "strong" (0.01 m – 0.03 m), "average" (0.04 m – 0.06 m) and "weak" (0.07 m – 0.1 m) turbulence, i.e. the strong, medium and weak intensity of turbulent distortions [17].

Calculation of the cross wind component is dependent on fluctuations in the power centers of gravity coordinates of the focal spot (centroid) measured S-H WFS. In this paper is provided an analysis of the nature of fluctuations of centroid

Downloaded From: http://proceedings.spiedigitallibrary.org/ on 11/24/2015 Terms of Use: http://spiedigitallibrary.org/ss/TermsOfUse.aspx

coordinates and, accordingly, the result of the reconstruction of the wavefront, arriving at the entrance aperture of the system, depending on the size of the lens array and on intensity of the turbulent distortions.

To evaluate the influence of the intensity of turbulent distortions and of the parameters of optical part on the correlation properties of S-H WFS measurements, we held a series of numerical experiments.

2. SCENARIO NUMERICAL EXPERIMENTS

The laser beam ($I = 10^5\,W/m^2$, $a_0 = 0.1m$, $\lambda = 0.633mkm$) passes through random turbulent screen (*1*), that is simulated by spectrum of von Karman. S-H WFS with lens array (*2*) captures the light field on Shack-Hartmann pattern (*3*). By the S-H WFS measurements (*4*) being reconstructed the wavefront (*5*). The calculations were performed on grid 512x512 pixels.

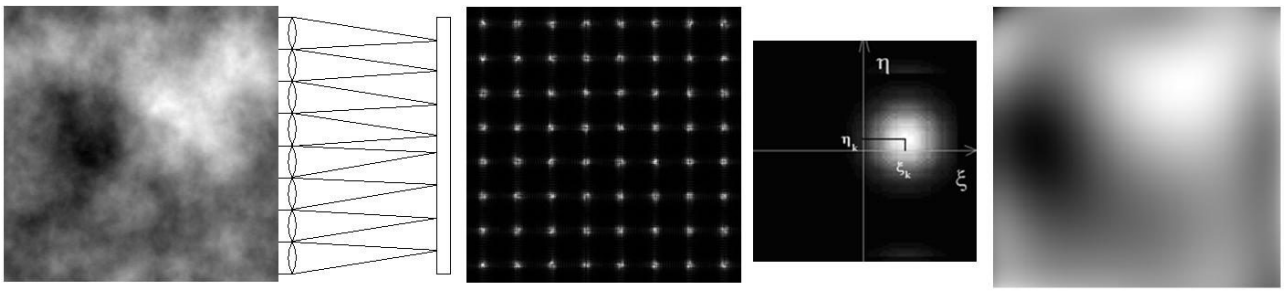

1 *2* *3* *4* *5*

Fig.2. Schematic representation of numerical experiment: 1 – the random turbulent screen; 2 – the lens array of S-H WFS; 3 – the Shack-Hartmann pattern in plane of camera; 4 – the coordinates of the centroid on a single Shack-Hartmann pattern; 5 – the reconstructed wavefront.

3. THE METHOD OF DETERMINATION OF WIND SPEED

Turbulence is moving in the transverse direction with the wind speed, according to the hypothesis of the "frozen" turbulence is a set of correlated random phase screens, each of which, starting from the second, is the result of the displacement in the transverse direction of the first screen, the simulated spectrum of von Karman. The spectrum of von Karman reflects the effects, associated with external and internal scale irregularities for the spectral density of fluctuations of the refractive index. This model has been used to create a numerical model of turbulence [9]:

$$\Phi_n(\vec{æ}) = 0{,}489 r_0^{-5/3} (\vec{æ}_0^2 + \vec{æ}^2)^{-11/6} \exp(-\vec{æ}^2 / \vec{æ}_m^2), \qquad (2)$$

where $\vec{æ}_m = 5.92/l_0, \vec{æ}_0 = 2\pi/L_0; L_0, l_0$ the external and internal scale of inhomogeneities. Experiments: $L_0 = 10\,m$; $l_0 = 1\,mm$. The intensity of phase fluctuations is characterized by the Fried's length: $r_0 = \left(0{,}423\kappa^2 C_n^2 L\right)^{-3/5}$. The Fried's length is determined by the wave length of the radiation, the length of the path, the parameters of the atmosphere. From these parameters depend on also the phase fluctuations. The dispersion of phase fluctuations is given the Fried's equation [16]: $\sigma^2 = 1{,}013(D/r_0)^{5/3}$, where D – the diameter of aperture.

The transverse component of the wind speed (the average value) is proportional to the transfer of the light field in the distance S. The transfer is effected by the wind in the plane of lens array over a time period Δt, i.e. $v_x = S/\Delta t$, where $S = D \cdot (N_{lens} - 1)$ – the distance between the lenses being analyzed; N_{lens} – the number of lenses in the line

Downloaded From: http://proceedings.spiedigitallibrary.org/ on 11/24/2015 Terms of Use: http://spiedigitallibrary.org/ss/TermsOfUse.aspx

matrix of Shack-Hartmann pattern. The transfer time is defined as the ratio of the number of displacements of turbulent screen N_{scr} over a period $T = 1/f$ to frequency camera f, i.e. $\Delta t = N_{scr}/\nu$.

The calculation of the transverse component of the wind speed is based on the definition of a linear relationship between the sampling time coordinates ξ two columns from a set of Shack-Hartmann pattern. Focal spots on Shack-Hartmann pattern correspond to the elements of the matrix. Each column consists of N_{lens} focal spots. The dependence is expressed by the linear correlation coefficient [18].

In determining of the speed of cross wind transport advisable to use a differential approach [19], since the displacement of the image, detects the jitter meter can be much greater than the displacement caused by atmospheric turbulence. The differential method is used in the calculation of the difference between elements of adjacent rows of matrix C_ξ. The matrix C_ξ is formed by the offset of centroids values of measured wavefront relative to a reference. The rows and columns of the matrix are numbered from top to bottom and left to right, respectively. Wind speed is determined by the analysis of the matrix C_ξ. This method of determining wind speed could be in the form of the following algorithm:

1. The calculation of the correlation coefficients of elements of each column of the last frame on the elements of all the columns of all the previous frames in the time T, corresponding to the length of the sample N, the time T is equal to the time of transfer "frozen" turbulence at the minimum wind speed, measured according to the device;

2. The definition of a pair of columns with a maximum value of correlation coefficients $R_{\xi\xi}$;

3. The difference between the numbers of columns times multiplied by the size of the input subaperture corresponding to the distance and direction that are "frozen" for the heterogeneity of time, expressed a number of frames until the exercise maximum correlation.

The equation for determining the current value of the instantaneous speed is as follows:

$$v_x = h \cdot (n_{final} - n_{corr}) / (N_{corr} \cdot \Delta t), \tag{3}$$

where h – the step on the input subaperture; n_{final} – the column number of the last frame N_{final}, forming a pair with the maximum value of correlation coefficient; n_{corr} – the column number of frame N_{corr}, forming a pair with the maximum value of correlation coefficient with respect to the column n_{final}, N_{corr} – the frame number to the columns with the maximum value of correlation coefficient correlation with respect to the last frame. There Δt – the time between frames.

The wind speed in the numerical experiment was set shifting sequence turbulent screen along the plane of the lens array. Table 1 shows the offset of shifts of the turbulent screen in pixels and the speed corresponding to this shift:

x, pxl	4	8	16	32	64
$v_x, m/s$	0,0625	0,125	0,25	0,5	1

Table 1. Results of numerical simulation.

The shift of turbulent screen occurred only on the "x" component, so the value of the components of "y" is not taken into account.

4. RESULTS AND DISCUSSION

In figures 3 – 4 it shows the profiles of the phase distribution of the initial wavefront and of the reconstructed wavefront for different values of the Fried's length, and also for different size of lens array.

Downloaded From: http://proceedings.spiedigitallibrary.org/ on 11/24/2015 Terms of Use: http://spiedigitallibrary.org/ss/TermsOfUse.aspx

The figure shows seen that in the center of the grid 512x512 the profiles of the reconstructed wavefront for sensors with different sizes of array and various modes of turbulence profiles at the center of reconstruction have a linear plot. On the periphery of the reconstructed phase distribution profiles have a significant variation, which may be due to the algorithm for the reconstruction of the wavefront by Zernike's polynomials, in particular the contribution of each of the Zernike's polynomials. This is clearly exemplified by the fourth Zernike's polynomial – the defocusing (Fig. 5).

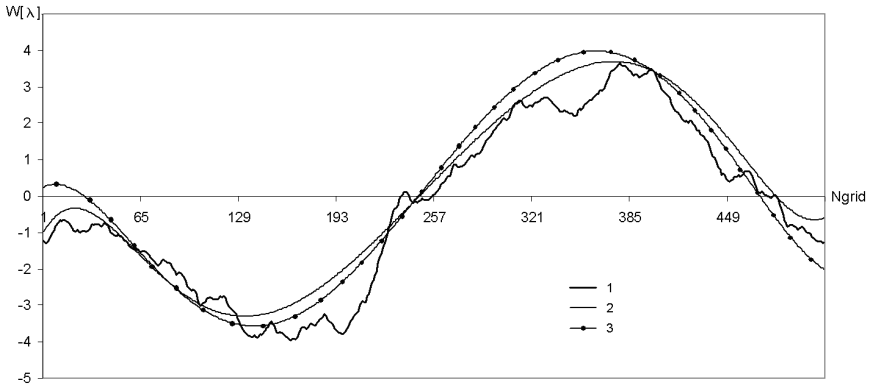

Fig.3. Profiles of phase distributions $W(x, y)$ in λ: Line 1 – the wavefront in the input aperture of the system, $r_0 = 0{,}05$ m; 2, 3 – the results of reconstruction by S-H SWF with a number lens 8x8 and 16x16, respectivelyOpto-electronic scheme of the S-H WFS.

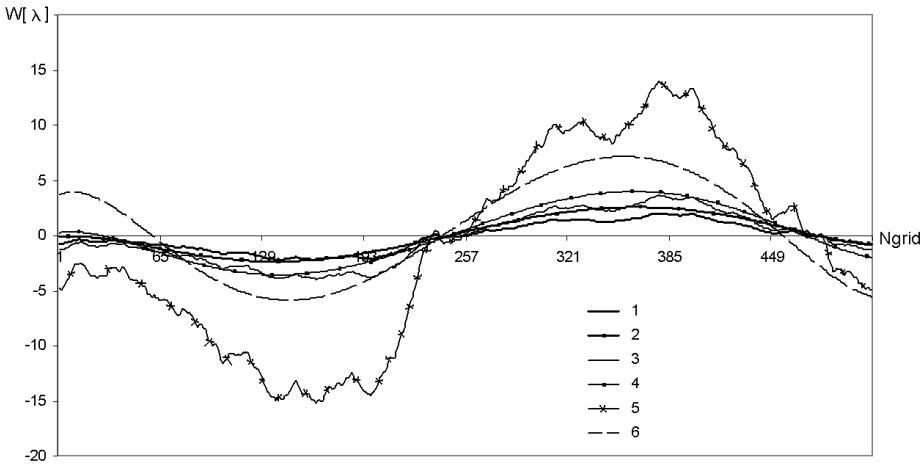

Fig.4. Profiles of the phase distribution $W(x, y)$ in λ, where the 1, 3, 5 – the random turbulent screen: 2, 4, 6 – the results of reconstruction, depending on the intensity of turbulent distortions: $r_0 = 0{,}1$ m (Lines 1,2); $r_0 = 0{,}05$ m (Lines 3, 4); $r_0 = 0{,}01$ m (Lines 5 and 6).

Downloaded From: http://proceedings.spiedigitallibrary.org/ on 11/24/2015 Terms of Use: http://spiedigitallibrary.org/ss/TermsOfUse.aspx

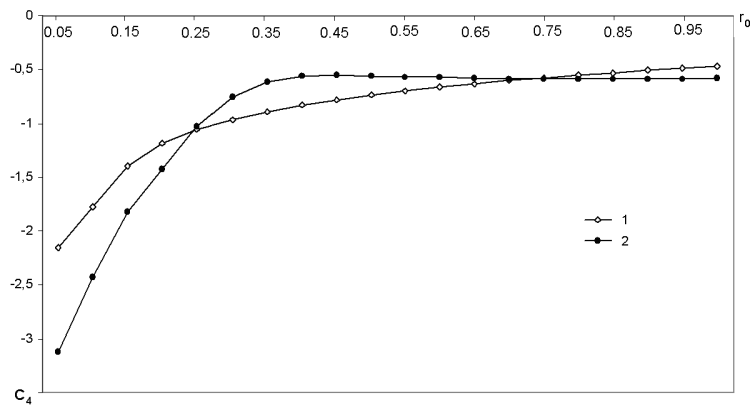

Fig.5. The changing of the focus (c_4) in the expansion of the wavefront by Zernike's polynomials, is depending on the Fried's length. Line 1 corresponds to the size of lens array 16x16; 2 – 8x8.

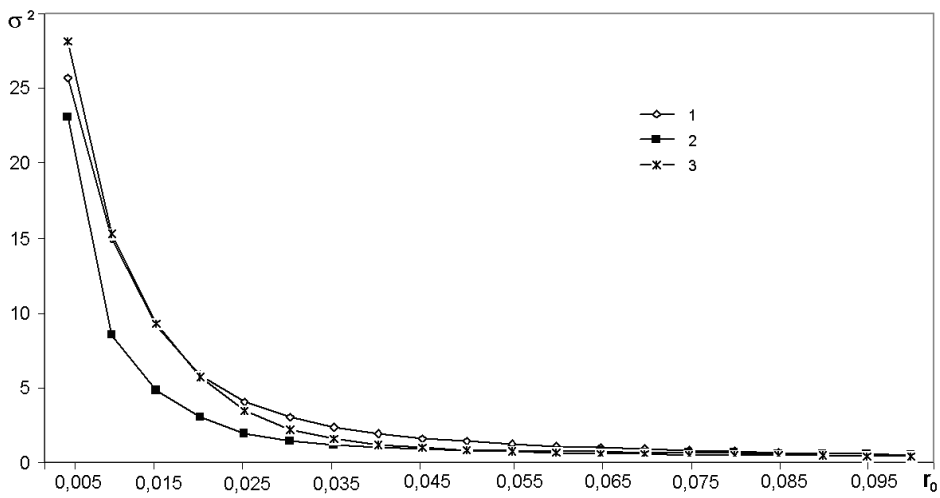

Fig.6. The dispersion between the phase distribution of the random turbulent screen at the entrance aperture of the system and the result of its reconstruction, is depending on the Fried's length. Line 1 corresponds to the size of lens array: 16x16; 2 – 8x8; 3 – to value of $(r_0)^{-5/3}$.

Fig. 6 that with increasing of the Fried's length the dispersion between the phase distribution of the random turbulent screen at the entrance aperture of the system and the result of its reconstruction varies in proportion to the Fried's equation: $\sigma^2 = 1{,}013(D/r_0)^{-5/3}$. This equation describes the amplitude of the phase oscillation in each area of the cross section of the beam relative to the mean phase value. It can be concluded that this dependence varies for different parameters of lens array. If there are the S-H WFS with a number lens 16x16 can be conclude, that the result of reconstruction is almost the same as the Fried's equation.

In table it shows the dispersion of the reconstructed wavefront depending on the serial number of the turbulent screen: N_{screen} . S-H WFS with the size of lens array 8x8 has a smaller value of the dispersion of the reconstructed wavefront with respect to the original wavefront than S-H WFS with the size of lens array 16x16.

Downloaded From: http://proceedings.spiedigitallibrary.org/ on 11/24/2015 Terms of Use: http://spiedigitallibrary.org/ss/TermsOfUse.aspx

	N_{screen}						
S-H SWF	1	2	3	4	5	6	7
8*8	,92484	1,22331	1,34091	2,35304	2,79471	0,95774	0,98821
16*16	,64326	2,03549	1,92569	3,03644	3,37434	3,21201	1,72879

Table 2. The dispersion of the reconstructed wavefront for S-H WFS with the size of lens array: 8x8 or 16x16.

Both sensors analyzed the wavefront with dimension 512x512. The number of lenses in a array is varied: 8x8 and 16x16, and is changed the size of each subaperture: 64x64 and 32x32 pixels, respectively. Thus, the first sensor had fewer subapertures with greater dimension than the second. The dimension of a array is equal to the number of the local areas of measured wavefront. On the other hand, the increasing the dimension of the array leads to a decrease in the area of the focal spot in the recording plane and, accordingly, is reduced the tilt angle of the light field, which is accompanied by different contributions of Zernike's polynomials in the reconstructed wavefront.

In figures 7 - 9 it shows the results of evaluation of the correlation properties of the sensor measurements, depending on the size of lens array, the frequency of image registration and the intensity of turbulent distortions

Fig. 7 shows the results of numerical experiments, analyzing the correlation field $R_{\xi}(x)$ depending on the size of the lens array: 8x8 and 16x16. The set of N_{scr} correlated random phase screen obtained as a result of displacement in the transverse direction of propagation of the laser beam on the first screen, four pixels, which corresponds to an average speed of the cross wind transport turbulent distortions $v_x = 0{,}0625 m/s$, according to the algorithm described above.

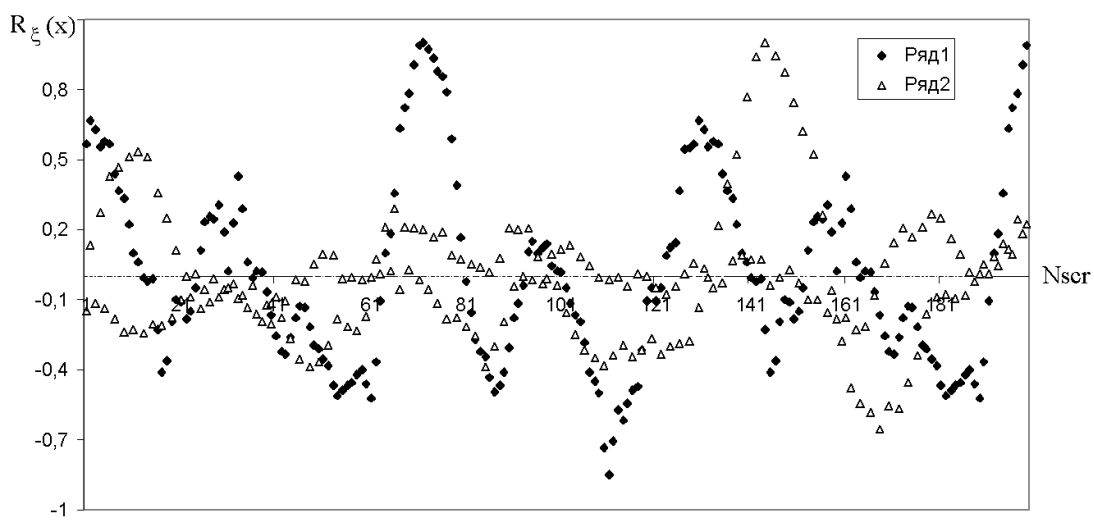

Fig.7 The correlation field $R_{\xi}(x)$ depending on the size of the lens array: series 1 corresponds to the number subapertures 8x8; 2 – 16x16.

The correlation field for the sensor with the lens array 8x8 differs from the correlation field calculated for the sensor with the lens array 16x16. The number of screens correlated between the maximum value $R_{\xi}(x)$ for the sensor with a number subapertures 8x8 smaller than for the sensor with a number subapertures 16x16.

There was also a calculation of the cross wind transport for the different variants of the intensity of turbulent distortions.

Downloaded From: http://proceedings.spiedigitallibrary.org/ on 11/24/2015 Terms of Use: http://spiedigitallibrary.org/ss/TermsOfUse.aspx

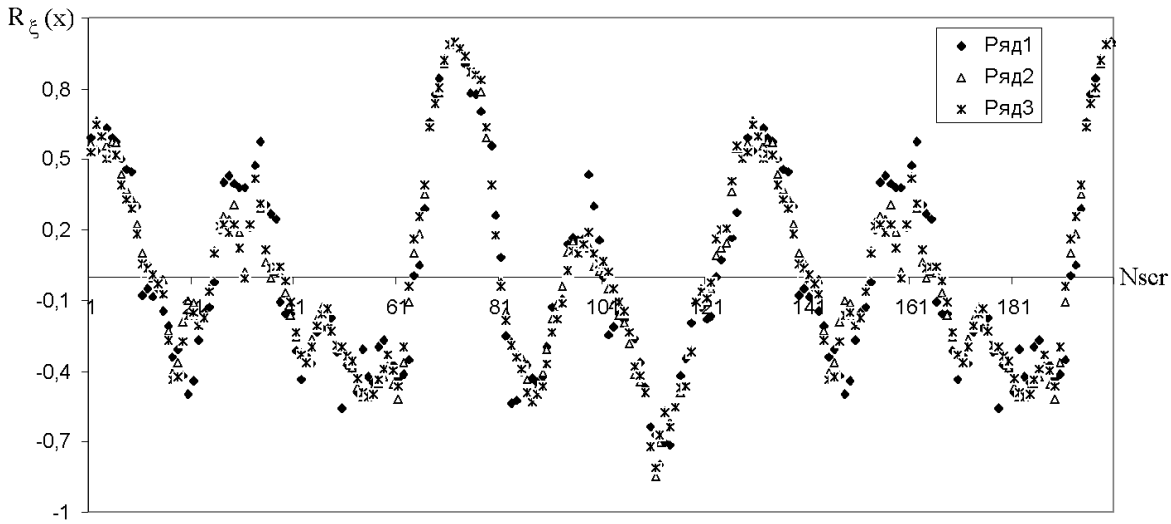

Fig.8. The correlation field $R_\xi(x)$ depending on the intensity of turbulent distortions: Line 1 corresponds to $r_0 = 0{,}01$ m; 2 – $r_0 = 0{,}05$ m; 3 – $r_0 = 0{,}1$ m

The correlation field $R_\xi(x)$ for a "strong" turbulence is significantly different from the correlation fields for the "medium" and "weak" turbulence. For the "medium" and "weak" turbulence the correlation fields differ slightly. The shift has also been the turbulent screen to four pixels, which corresponds to an average speed of cross wind transport of turbulent distortions $v_x = 0{,}0625 m/s$, according to the algorithm described above.

Figure 9 shows the correlation field $R_\xi(x)$ depending on the frame rate of the camera, which is a numerical experiment simulated the number of pixels the screen moves turbulent (2) in the direction along the lens array. The shift of eight pixels corresponds to the frame rate camera, twice the frequency of the displacement of turbulent screen into four pixels. The correlation fields considered different frequencies: the field correlation with higher frame rate camera is characterized by two times fewer screens correlated between the maximum value $R_\xi(x)$ relative to the field of correlation with a lower frequency.

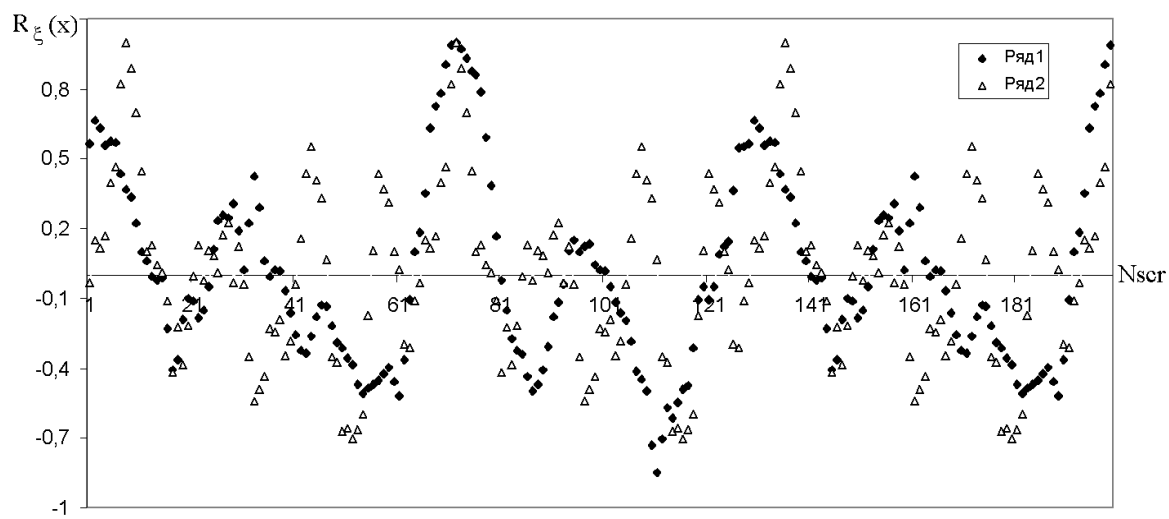

Fig.9. The field correlation $R_\xi(x)$ depending on the frequency of frames: 1 corresponds to the shift of the first screen (2) on four pixels; 2 - the result of the displacement on eight pixels.

Downloaded From: http://proceedings.spiedigitallibrary.org/ on 11/24/2015 Terms of Use: http://spiedigitallibrary.org/ss/TermsOfUse.aspx

CONCLUSION

Task of S-H WFS in adaptive optical systems are usually is to manage correction device based on the information about the intensity of optical radiation, which sensor is converted into a two-dimensional phase distribution. The data measured of S-H WFS have correlation properties [13 - 15], which also allows them to calculate the parameters of turbulent distortions of the light field and the speed of the cross wind transport of turbulent distortions. Within these parameters, the calculation control actions corrective mirror [20] will allow to take into account the evolution in time and phase [11, 12], thereby to increase the effectiveness of correction of turbulent distortions by AOS in transmitting and receiving optical radiation at large distances in astronomy, as well as in the transmission energy in the face the atmosphere in telecommunications and laser systems.

S-H WFS with different parameters of lens array sheet and a receiving device, with the coordinates of the centroids calculated by another algorithm different from the algorithm for the weighted centers of gravity (1), as well as other atmospheric turbulence limits of applicability of the algorithm require separate consideration in each case.

REFERENCES

[1] Lukin V.P. Adaptive optics in the formation of optical beams and images, Physics –Uspekhi, 57(6), 556-592(2014).

[2] Lukin V.P., Botygina N.N., Emaleev O.N., Korol'kov V.P., Lavrinova L.N., Nasyrov R.K., Poleshchuk A.G., Cherkashin V.V. Shack-Hartmann sensor based on a low-aperture off-axis diffraction lens array, Optoelectronics, Instrumentation and Data, 45(2), 88-98(2009).

[3] Rukosuev A.L., Kudryashov A.V., Lylova A.N., Samarkin V.V., Sheldakova Yu.V. Adaptive optical system for real-time wavefront correction, Atmospheric and oceanic optics, 28(2), 189-195(2015).

[4] Artyshchenko S.V., Golovinski P.A., Chernov R.A. Reconstruction of the wavefront phase with the use of a complex neural network, Atmospheric and oceanic optics, 27(10), 932-936(2014).

[5] Lukin V.P., Botygina N.N., Gladkikh V.A., Emaleev O.N., Konyaev P.A., Odintsov S.L., Torgaev A.V. Comparative measurements of atmospheric turbulence level with optical and acoustic meters, Atmospheric and oceanic optics, 28(2), 163-166(2015).

[6] Antoshkin L.V., Lavrinov V.V., Lavrinova L.N., Lukin L.V. Measurement of cross wind transfer of atmospheric turbulence on basis of Shack-Hartman sensor, Mountain information analytical journal, 17(12), 129-133(2009).

[7] Voitsekhovich V.V., Orlov V.G., Cuevas S. Simulations of turbulent-induced log-amplitude fluctuations: the Karhunen-Loeve approach, Atmospheric and oceanic optics, 9(11), 957-958(1996).

[8] Aksenov V.P., Isaev Yu.N. Optimal mode expansion of phase reconstructed from measurements of wavefront tilts in a turbulent atmosphere. Part I. Aberration representation in the Karhunen-Loeve-Obukhov basis, Atmospheric and oceanic optics, 7(7), 506-509(1994).

[9] Vorontsov M.A., Shmal'gauzen V.I. Principles of adaptive optics, Moscow, Nauka, 336 (1985).

[10] Lavrinov V.V., Lavrinova L.N., Tuev M.V. Numerical simulation of the algorithm to compute the voltage control for the flexible mirror depending on the presentation of information on the wavefront , Atmospheric and Oceanic optics, 27(10), 925-931 (2014).

[11] Lukin V.P. Dynamic characteristics of adaptive optics systems, Atmospheric and oceanic optics, 23(11), 1027-1035(2010).

[12] Lavrinov V.V., Kopylov E.A., Lukin L.V. The development of effective control algorithms with adaptive optical systems for astronomical instruments and laser optoelectronic systems, Proceedings of V Scientific Conference OAO "GSKB "Almaz-Antey", 476-483(2014).

[13] Vernin J., Roddier F. Experimental determination of two-dimensional spatiotemporal power spectra of stellar light scintillation. Evidence for a multilayer structure of the air turbulence in the upper troposphere, J. Opt. Soc. Am, 63, 270 – 273(1973).

[14] Roopashree M.B., Akondi Vyas, B. Raghavendra Prasad Real-time wind speed measurement using wavefront sensor data, Proc. of SPIE, 7588, 0A-2-0A-12(2010).

Downloaded From: http://proceedings.spiedigitallibrary.org/ on 11/24/2015 Terms of Use: http://spiedigitallibrary.org/ss/TermsOfUse.aspx

[15] Schock M., Spillar S.J. Measuring wind speeds and turbulence with a wave-front sensor, Optics Letters, 23(3), 150-152(1980).
[16] Tokovinin A. Measurement of seeing and the atmospheric time constant by differential scintillations, Applied Optics, 41, 957–964(2002).
[17] Lavrinova L.N., Lukin V.P. Adaptive correction of thermal and turbulent distortions of laser radiation by deformable mirror, Tomsk, Publishing House of the Institute of Atmospheric Optics SB RAS, 152(2008).
[18] Taylor John R. An introduction to error analysis, University Science Books Mill Valley, California, 272(1982).
[19] Antoshkin L.V., Lavrinov V.V., Lavrinova L.N., Lukin L.V. Differential method at measuring of turbulence parameters and wind speed by wavefront sensor, Atmospheric and Oceanic optics, 21(1), 75-80(2008).
[20] Rukosuev A.L., Kudryashov A.V., Lylova A.N., Samarkin V.V., Sheldakova Yu.V. Adaptive optical system for real-time wavefront correction, Atmospheric and oceanic optics, 28(2), 189-195(2015).

Downloaded From: http://proceedings.spiedigitallibrary.org/ on 11/24/2015 Terms of Use: http://spiedigitallibrary.org/ss/TermsOfUse.aspx